Recent Progress on Inclusive Quarkonium Production and Polarization

Xiang-Peng Wang (王翔鹏)

华中师范大学

2026年4月26日

第八届全国重味物理与量子色动力学研讨会 | 重庆 | 2026年4月24–28日

Contents

1. Introduction of and Review

Quarkonium; NRQCD factorization formalism; heavy quark spin symmetry and power counting; review on testing universality of the LDMEs

Quarkonium: A multi-scale system

Quarkonium: heavy quark-antiquark bound states – $J/\psi, \Upsilon, \chi_{cJ}, \chi_{bJ}, B_c$ ...

QCD version of the hydrogen atom: the simplest QCD bound state.

Why quarkonium?

- Excellent probe of PDFs, GPDs, TMDs, QGP, nucleon helicity structure...
- Ideal system to study both perturbative and nonperturbative aspects of QCD.

Default EFT for quarkonium

- Quarkonium is a nonrelativistic system.
- Nonrelativistic QCD (NRQCD) is the default effective theory .

Caswell & Lepage, PLB 167 (1986) 437–442

Typical scales (besides $\Lambda_{\rm QCD}$)

m_Q	$m_c \sim 1.5$ GeV, $m_b \sim 4.75$ GeV
$m_Q v$	typical heavy-quark momentum
$m_Q v^2$	kinetic energy and binding energy
v	typical heavy-quark velocity in the quarkonium rest frame

$v_c^2 \sim 0.3$ for charmonium

$v_b^2 \sim 0.1$ for bottomonium

NRQCD factorization

NRQCD factorization is the most prominent approach to describe quarkonium production.

Bodwin, Braaten & Lepage, PRD 51, 1125 (1995), 3100+ citations.

$$\sigma_{Q+X} = \sum_n \hat{\sigma}\left(ij \to Q\bar{Q}(n) + X\right) \langle O^Q(n) \rangle, \tag{1}$$

$n = {}^{2S+1}L_J^{[1/8]}$ labels the quantum state of the heavy quark anti-quark pair.

SDCs & LDMEs

- SDCs ($\hat{\sigma}$): short-distance coefficients, organized in the α_s expansion.
- LDMEs ($\langle O^Q(n) \rangle$): long-distance matrix elements, supposed to be universal, organized in the v^2 expansion.
- For $J/\psi, \Upsilon$, the ${}^3S_1^{[1]}$, ${}^3S_1^{[8]}$, ${}^1S_0^{[8]}$, and ${}^3P_J^{[8]}$ channels are usually included.

About NRQCD factorization

- NRQCD factorization is still a conjecture.
- Violations were found in specific inclusive cases, for instance processes involving two or more quarkonia.

He, Kniehl & **XPW**, PRL 121 (2018) 17, 172001

LDMEs

Spin-1 S-wave quarkoniumLDME definitions ($V = J/\psi, \psi(2S), \Upsilon(nS)$) :

$$\langle O^V(^3S_1^{[1]})\rangle = \langle\Omega|\chi^\dagger\sigma^i\psi\mathcal{P}_{V(\boldsymbol{P}=\boldsymbol{0})}\psi^\dagger\sigma^i\chi|\Omega\rangle, \tag{2a}$$

$$\langle O^V(^3S_1^{[8]})\rangle = \langle\Omega|\chi^\dagger\sigma^i T^a\psi\Phi_\ell^{\dagger ab}\mathcal{P}_{V(\boldsymbol{P}=\boldsymbol{0})}\Phi_\ell^{bc}\psi^\dagger\sigma^i T^c\chi|\Omega\rangle, \tag{2b}$$

$$\langle O^V(^1S_0^{[8]})\rangle = \langle\Omega|\chi^\dagger T^a\psi\Phi_\ell^{\dagger ab}\mathcal{P}_{V(\boldsymbol{P}=\boldsymbol{0})}\Phi_\ell^{bc}\psi^\dagger T^c\chi|\Omega\rangle, \tag{2c}$$

$$\begin{aligned}\langle O^V(^3P_0^{[8]})\rangle = \frac{1}{3}\langle\Omega|\chi^\dagger(-\tfrac{i}{2}\overleftrightarrow{\boldsymbol{D}}\cdot\boldsymbol{\sigma})T^a\psi\Phi_\ell^{\dagger ab}\mathcal{P}_{V(\boldsymbol{P}=\boldsymbol{0})}\\ \times\Phi_\ell^{bc}\psi^\dagger(-\tfrac{i}{2}\overleftrightarrow{\boldsymbol{D}}\cdot\boldsymbol{\sigma})T^c\chi|\Omega\rangle,\end{aligned} \tag{2d}$$

Operator ingredients

- $\mathcal{P}_{V(\boldsymbol{P})} = \sum_X |V+X\rangle\langle V+X|$:
  projector onto states containing the observed quarkonium.
- Φ_ℓ: path-ordered Wilson line required by gauge invariance.

Color-singlet (CS) and color-octet (CO)

- CS LDMEs can be related to the quarknoum wave-function at origin – $|R(0)|^2$.
- CO LDMEs, not yet available through lattice QCD.
- In practice, CO LDMEs are extracted from fits to experimental data.

Heavy quark spin symmetry (HQSS)

Spin-1 S-wave quarkonium V

For $V = J/\psi, \Upsilon, \cdots$, HQSS gives

$$\langle O^V(^3P_J^{[8]})\rangle = (2J+1)\langle O^V(^3P_0^{[8]})\rangle(1+O(v^2)). \tag{3}$$

Each spin-1 S-wave quarkonium inclusive production usually needs three independent CO LDMEs:

$$\langle O^V(^3S_1^{[8]})\rangle, \quad \langle O^V(^1S_0^{[8]})\rangle, \quad \langle O^V(^3P_0^{[8]})\rangle.$$

η_c-J/ψ relations from HQSS

$$\langle O^{\eta_c}(^1S_0^{[1]}/^1S_0^{[8]})\rangle = \frac{1}{3}\langle O^{J/\psi}(^3S_1^{[1]}/^3S_1^{[8]})\rangle(1+O(v^2)), \tag{4}$$

$$\langle O^{\eta_c}(^3S_1^{[8]})\rangle = \langle O^{J/\psi}(^1S_0^{[8]})\rangle(1+O(v^2)), \tag{5}$$

$$\langle O^{\eta_c}(^1P_1^{[8]})\rangle = 3\langle O^{J/\psi}(^3P_0^{[8]})\rangle(1+O(v^2)). \tag{6}$$

These relations allow a combined J/ψ-η_c fit to constrain the three J/ψ color-octet LDMEs.

High-p_T power counting for J/ψ production

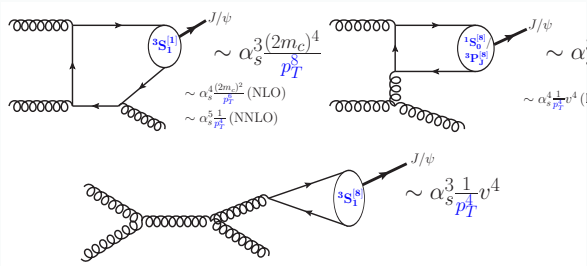

At LO, only $^3S_1^{[8]}$ gives leading power (LP) of p_T; at NLO, $^1S_0^{[8]}$ and $^3P_J^{[8]}$ also enter at LP.

- At high p_T, p_T power counting dominates over α_s and v^2 counting.
- At LO, only $^3S_1^{[8]}$ gives the LP contribution $(1/p_T^4)$, leading to strong transverse polarization and the J/ψ polarization puzzle.
- NLO is essential, since the dominant LP contributions from $^1S_0^{[8]}$ and $^3P_J^{[8]}$ first enter at this order.

CS contribution remains small even at NNLO; Ma, Wang, Chao, PRD 84, 114001 (2011).

Why the existing J/ψ LDME fits look incompatible

Two fitting philosophies

- **Global fit:** include pp, $p\bar{p}$, γp, $\gamma\gamma$, and e^+e^- data with $p_T > 3$ GeV. Butenschön & Kniehl, PRD 84, 051501 (2011)
- **High-p_T hadroproduction fits:** fit only hadroproduction data with $p_T > 7$ GeV.
  Ma, Wang & Chao, PRL 106, 042002 (2011); Zhang et al., PRL 114, 092006 (2015); Feng et al., PRD 99, 014044 (2019)

Table 1: Selected representative fitting results in units of 10^{-2} GeV^3.

Group	$\langle O^{J/\psi}(^3S_1^{[8]})\rangle$	$\langle O^{J/\psi}(^1S_0^{[8]})\rangle$	$\langle O^{J/\psi}(^3P_0^{[8]})\rangle/m_c^2$
Butenschön et al.	0.168 ± 0.046	3.04 ± 0.35	−0.404 ± 0.072
Chao et al. set 1	0.05	7.4	0
Chao et al. set 2	1.11	0	1.89
Zhang et al.	1.0 ± 0.3	0.74 ± 0.3	1.7 ± 0.5
Feng et al.	0.117 ± 0.058	5.66 ± 0.47	0.054 ± 0.005

Key point: high p_T J/ψ hadroproduction data alone can only constrain two linear combinations of the 3 CO LDMEs.

Score card of fittings

Table 2: Tests of the J/ψ LDME fits against high-p_T pp and low-p_T γp, e^+e^-, $\gamma\gamma$ data.

Group	pp (p_T in fit)	pp (pol.)	pp (η_c)	$J/\psi + Z$	e^+e^-	γp	$\gamma\gamma$
global fit with $p_T > 3$ GeV							
Butenschön et al.	✓ ($p_T > 3$GeV)	✗	✗	✗	✓	✓	✗
high-p_T hadroproduction fits with $p_T > 7$ GeV							
Chao et al. set 1	✓ ($p_T > 7$GeV)	✓	✗	-	✗	✗	-
Chao et al. set 2	✓ ($p_T > 7$GeV)	✓	✓	-	✗	✗	-
Zhang et al. $+\eta_c$	✓ ($p_T > 7$GeV)	✓	✓	-	✗	✗	-
Feng et al.	✓ ($p_T > 7$GeV)	✓	✗	-	✗	✗	-

How should we read this table?

- High-p_T hadroproduction fits fail systematically in relatively low p_T J/ψ production from γp and e^+e^-.
- Global fit fails in polarization descriptions, even fails for low p_T $\gamma\gamma$ data.
- Simplest explanation: NRQCD factorization fails at low p_T. (Talk by Bodwin in Oct. 2024 at Cornell.)

2. Potential NRQCD in Inclusive Quarkonium Production

pNRQCD relates LDMEs among different quarkonia through gluonic correlators and makes NRQCD factorization more predictive.

Spin-1 S-wave LDMEs in pNRQCD

- Based on potential NRQCD (pNRQCD), we have (up to $O(1/N_c^2, v^2)$ corrections),

  Brambilla, Chung, Vairo & **XPW**, PRD105, L111503 (2022); JHEP 03 (2023) 242

$$\langle \mathcal{O}^V(^3S_1^{[1]})\rangle = 2N_c \times \frac{3|R_V^{(0)}(0)|^2}{4\pi}, \tag{7a}$$

$$\langle \mathcal{O}^V(^3S_1^{[8]})\rangle = \frac{1}{2N_c m^2}\frac{3|R_V^{(0)}(0)|^2}{4\pi}\mathcal{E}_{10;10}, \tag{7b}$$

$$\langle \mathcal{O}^V(^1S_0^{[8]})\rangle = \frac{1}{6N_c m^2}\frac{3|R_V^{(0)}(0)|^2}{4\pi}c_F^2\mathcal{B}_{00}, \tag{7c}$$

$$\langle \mathcal{O}^V(^3P_0^{[8]})\rangle = \frac{1}{18N_c}\frac{3|R_V^{(0)}(0)|^2}{4\pi}\mathcal{E}_{00}, \tag{7d}$$

- c_F is the NRQCD (HQET) matching coefficient; $R_V^{(0)}(0)$ is the wave-function at the origin,
- $\mathcal{E}_{10;10}$, $\mathcal{B}_{00}$, and $\mathcal{E}_{00}$ are flavor independent gluonic correlators of mass dimension 2.

Gluonic correlators

$$\mathcal{E}_{10;10} = \Big| d^{dac} \int_0^\infty dt_1\, t_1 \int_{t_1}^\infty dt_2\, g E^{b,i}(t_2) \times \Phi_0^{bc}(t_1;t_2) g E^{a,i}(t_1) \Phi_0^{df}(0;t_1) \Phi_\ell^{ef} |\Omega\rangle \Big|^2, \tag{8a}$$

$$\mathcal{B}_{00} = \Big| \int_0^\infty dt\, g B^{a,i}(t) \Phi_0^{ac}(0;t) \Phi_\ell^{bc} |\Omega\rangle \Big|^2, \tag{8b}$$

$$\mathcal{E}_{00} = \Big| \int_0^\infty dt\, g E^{a,i}(t) \Phi_0^{ac}(0;t) \Phi_\ell^{bc} |\Omega\rangle \Big|^2, \tag{8c}$$

where $\Phi_0(t,t') = \mathcal{P} \exp[-ig \int_t^{t'} d\tau\, A_0^{\mathrm{adj}}(\tau, \mathbf{0})]$ is a Schwinger line.

- Gluonic correlators can be calculated using lattice QCD, especially within gradient flow formalism.
  Brambilla & **XPW**, JHEP 06 (2024) 210
- By evolving the scale of $\mathcal{E}_{10;10}$, $\mathcal{B}_{00}$, and $\mathcal{E}_{00}$ from charm mass scale m_c to bottom mass scale m_b, we can related CO LDMEs between $\psi(nS)$ and $\Upsilon(nS)$.
- pNRQCD significantly reduces the number of independent CO LDMEs ($15 \to 3$).

pNRQCD predictive power

Cross section ratio $\psi(2S)/J/\psi$

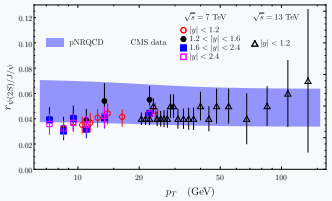

Cross section ratio $\Upsilon(3S)/\Upsilon(2S)$

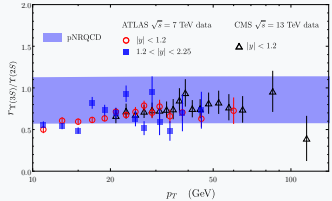

Figures from Brambilla, Chung, Vairo & **XPW**, JHEP 03 (2023) 242

- Left block: $\sigma[\psi(2S)]/\sigma[J/\psi]$ is fixed by the ratio $|R^{(0)}_{\psi(2S)}(0)|^2/|R^{(0)}_{J/\psi}(0)|^2$.
- Right block: the same pNRQCD relation predicts $\sigma[\Upsilon(3S)]/\sigma[\Upsilon(2S)]$.
- These ratios follow from NRQCD factorization and pNRQCD LDME relations without explicit perturbative calculations.

Score card of fittings - update 1

Table 3: Tests of the J/ψ LDMEs fits from high p_T pp, and low p_T γp, e^+e^-, $\gamma\gamma$ data.

Group	pp (p_T in fit)	pp (pol.)	pp (η_c)	$J/\psi + Z$	e^+e^-	γp	$\gamma\gamma$
global fit with $p_T > 3$ GeV							
Butenschön et al.	✓ ($p_T > 3\,\mathrm{GeV}$)	✗	✗	✗	✓	✓	✗
high-p_T hadroproduction fits with $p_T > 7$ GeV							
Chao et al. set 1	✓ ($p_T > 7\,\mathrm{GeV}$)	✓	✗	-	✗	✗	-
Chao et al. set 2	✓ ($p_T > 7\,\mathrm{GeV}$)	✓	✓	-	✗	✗	-
Zhang et al. $+\eta_c$	✓ ($p_T > 7\,\mathrm{GeV}$)	✓	✓	-	✗	✗	-
Feng et al.	✓ ($p_T > 7\,\mathrm{GeV}$)	✓	✗	-	✗	✗	-
pNRQCD high-p_T fits							
Brambilla et al.	✓ ($p_T > 5 \times 2m_Q$)	✓	✓	✓(?)	✗	✗	-

- Brambilla et al.: pNRQCD fit to the three gluonic correlators using high-p_T J/ψ, $\psi(2S)$, $\Upsilon(2S)$, and $\Upsilon(3S)$ data; it favors a small negative $\langle O^{J/\psi}(^1S_0^{[8]})\rangle$.
- Conflicts between the low-p_T and high-p_T descriptions still remain.

The remaining main conflicts/puzzles

Predictions with high-p_T fit

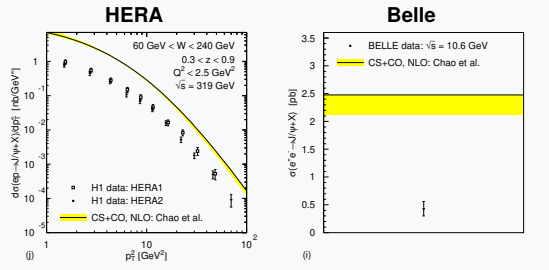

Predictions with global fit (low p_T cut)

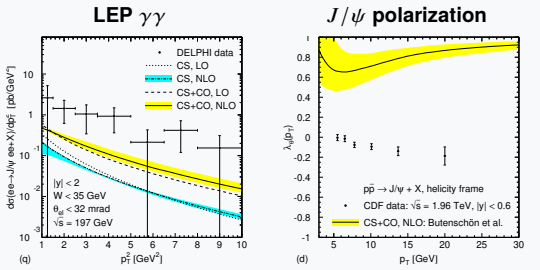

Figures from Butenschön & Kniehl, Mod.Phys.Lett. A 28 (2013) 1350027.

- Left block: the high-p_T fit overshoots the HERA and Belle data by factors of ~ 5–10.
- Right block: the global fit with a low-p_T cut still misses the LEP $\gamma\gamma$ cross section and the J/ψ polarization data.
- Together they expose the tension between high-p_T fits and low-p_T observables.

3. How Well Does NRQCD Factorization Work at NLO?

Let's systematically study inclusive quarkonium production in $pp, \gamma p, \gamma\gamma, e^+e^-$ collisions.

Our new fitting strategies and fitting results

- We combine LHC η_c and J/ψ data (42 data points) to fit 3 J/ψ CO LDMEs based on HQSS.
- We choose three different scale choices, $\mu_r = \mu_f = [\frac{1}{2}, 1, 2]m_T$, with the default scale choice $\mu_r = \mu_f = m_T$, where $m_T = \sqrt{4m_Q^2 + p_T^2}$;
- Systematically taking scale variations into account for the first time.
- $\psi(2S), \Upsilon(nS)$ CO LDMEs are related to those of J/ψ through pNRQCD relations. Feeddown from χ_{QJ} states are fitted from the measured data.

We obtain (in units of 10^{-2} GeV^3),

$\mu_r = \mu_f$	$\langle O^{J/\psi}(^3S_1^{[8]})\rangle$	$\langle O^{J/\psi}(^1S_0^{[8]})\rangle$	$\frac{\langle O^{J/\psi}(^3P_0^{[8]})\rangle}{m_c^2}$	$\frac{\chi^2_{\min}}{\text{d.o.f}}$
$m_T/2$	0.592 ± 0.057	-0.205 ± 0.196	0.697 ± 0.089	0.34
m_T	1.050 ± 0.121	0.068 ± 0.2489	1.879 ± 0.261	0.22
$2m_T$	1.382 ± 0.189	0.358 ± 0.303	3.270 ± 0.533	0.21

Fitting – η_c and J/ψ hadroproduction

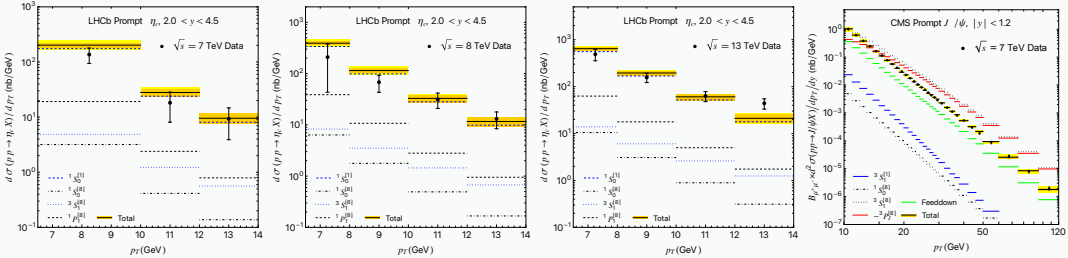

Left three panels: LHCb η_c production; right panel: CMS J/ψ production.
Inner orange band: $\mu_r = \mu_f = m_T$;
Outer yellow band : $\mu_r = \mu_f = m_T/2$ or $2m_T$.

- For η_c, the CS channel nearly saturates the data, pointing to a small HQSS-related $\langle O^{J/\psi}(^1S_0^{[8]})\rangle$.
- For prompt J/ψ, the fit is driven by a cancellation between the $^3S_1^{[8]}$ and $^3P_J^{[8]}$ channels; at NLO only their sum has physical significance due to mixing between these two channels.

Prediction – ATLAS J/ψ production at very high p_T

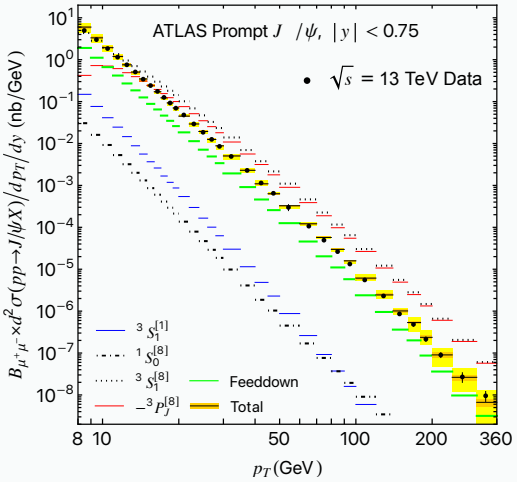

Excellent descriptions at very high p_T

- Excellent agreement persists up to the highest measured point, $p_T = 360\,\mathrm{GeV}$.
- Increasingly larger cancellation ($> 95\%$) at higher p_T indicates strong mixing.
- Large cancellation at higher p_T would lead to negative cross section predictions due to incomplete cancellation, refinements needed at higher p_T.

Chung, Kim & Lee, PRL 134, 071902 (2025);

Chen, Ma & Meng , PRD 108 (2023) 1, 014003.

Prediction – LHCb J/ψ production at low p_T

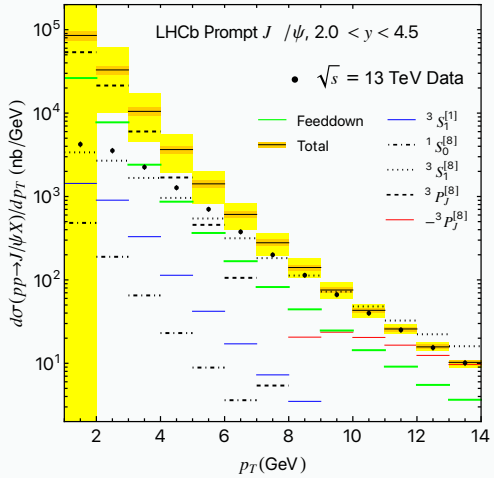

Fail at relatively low p_T

- The tension is concentrated in the region $p_T < 7\,\mathrm{GeV}$.
- We may need small-x resummation at this relatively low p_T region.

Ma & Venugopalan, PRL 113, 192301 (2014)

Prediction – ATLAS $\Upsilon(nS)$ production in pNRQCD

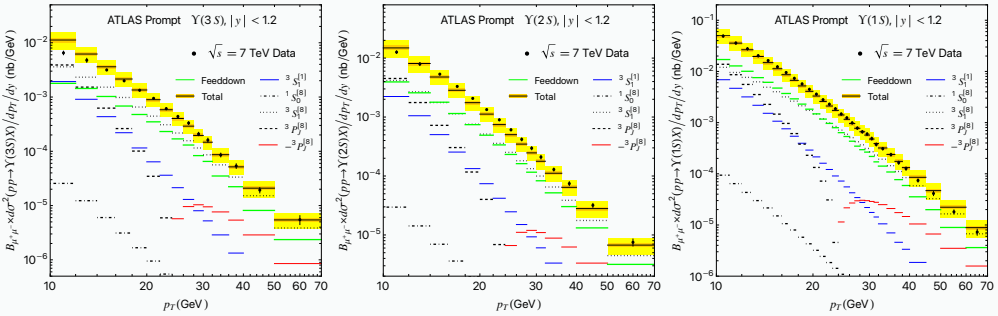

- Based on converting the fitted J/ψ LDMEs into those of $\Upsilon(nS)$ using relations from pNRQCD.
- $\Upsilon(1S), \Upsilon(2S), \Upsilon(3S)$ data well reproduced, highly nontrivial test of the pNRQCD relations.
- Cancellation between the $^3S_1^{[8]}$ and $^3P_J^{[8]}$ channels are weak due to suppressed soft radiations.

Prediction –J/ψ polarization

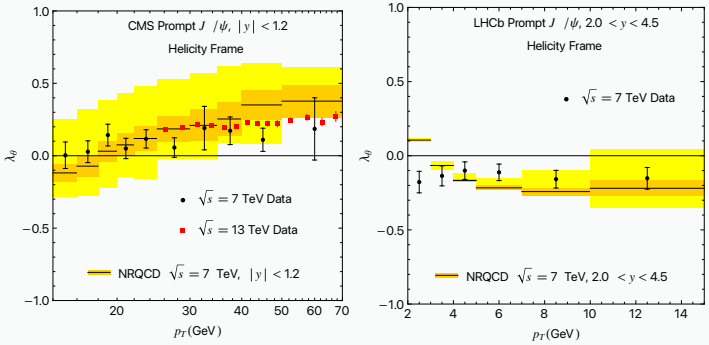

- In good agreement with the measurements and match the pattern that λ_θ turns from slightly negative at relatively low p_T to positive and converges to $\lambda_\theta \sim 0.3$ at high p_T.
- No polarization puzzle appears.

Prediction – ATLAS $J/\psi + Z$, single parton scattering (SPS)

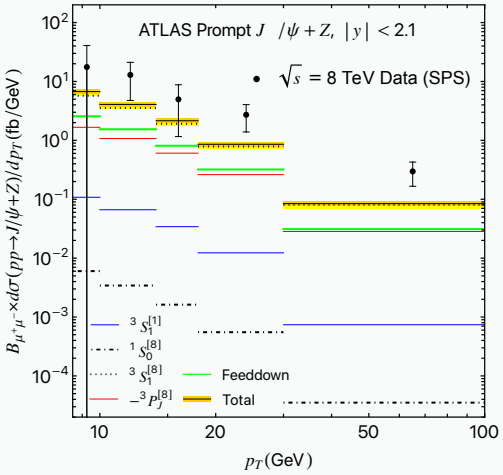

Tension in the highest p_T bins

- For the two highest p_T bins, predictions lie about $\sim 2\sigma$ below the data.
- Could the DPS contribution still be underestimated?

Prediction – LEP $\gamma\gamma \to J/\psi + X$

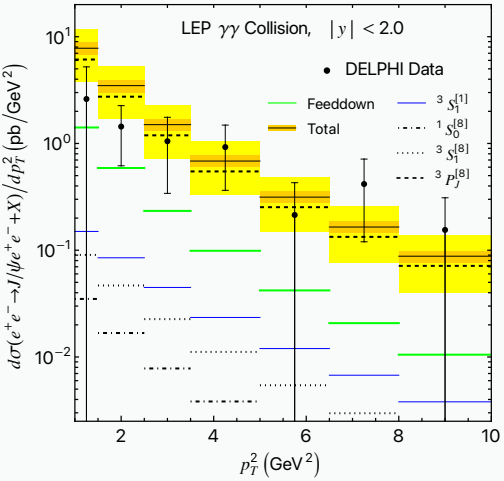

Good descriptions for low p_T data

- The CS contribution is far below the data.
- $^3P_J^{[8]}$ channels dominate.
- Very large uncertainties in the data, more precise measurements needed.

Prediction – HERA $\gamma p \to J/\psi + X$ ($0.1 < z < 0.6$)

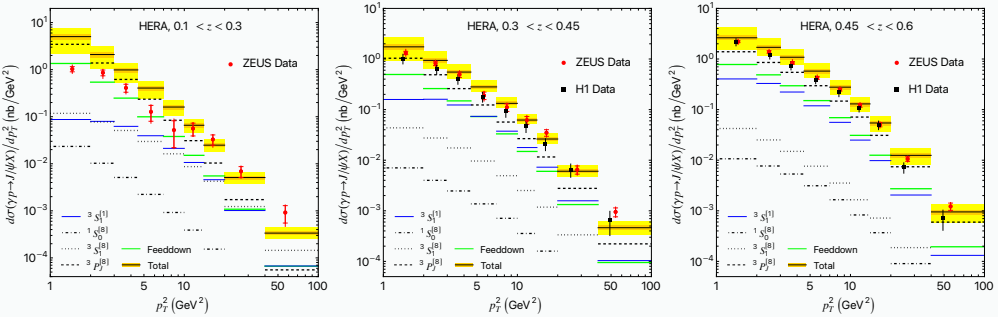

Figure 1: Prediction with divided z bins. Inelasticity $z = E_{J/\psi}/E_\gamma$ in the proton rest frame.

- For $0.1 < z < 0.6$, good description for all the data except for a few lowest p_T bins for $0.1 < z < 0.3$, where resolved photon ($gg \to J/\psi + X$, similar to hadroproduction) contribution dominates.

Prediction – HERA $\gamma p \to J/\psi + X$ ($0.6 < z < 0.9$)

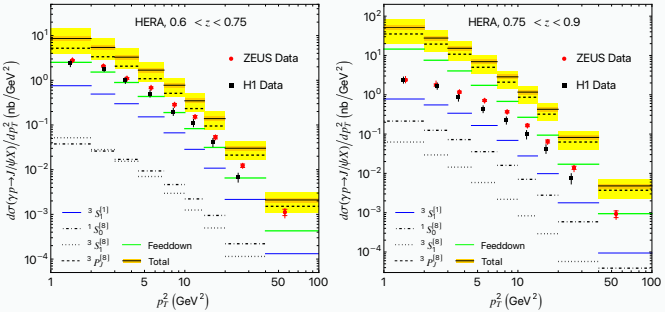

- Obviously overshoot the data, regardless of p_T.
- For $0.75 < z < 0.9$, predictions overshoot the data by factors of 5.2 to 20.
- $z \to 1$ corresponds to the endpoint region, where the NRQCD factorization may not be valid.

Beneke, Rothstein & Wise, PLB 408, 373 (1997).

Score card of fittings - update 2

Table 4: Tests of the J/ψ LDMEs fits from high p_T pp, and low p_T γp, e^+e^-, $\gamma\gamma$ data.

Group	pp (p_T in fit)	pp (pol.)	pp (η_c)	$J/\psi + Z$	e^+e^-	γp	$\gamma\gamma$
Butenschön et al.	✓ ($p_T > 3\,\mathrm{GeV}$)	✗	✗	✗	✓	✓	✗
Chao et al. set 1	✓ ($p_T > 7\,\mathrm{GeV}$)	✓	✗	-	✗	✗	-
Chao et al. set 2	✓ ($p_T > 7\,\mathrm{GeV}$)	✓	✓	-	✗	✗	-
Zhang et al. $+\eta_c$	✓ ($p_T > 7\,\mathrm{GeV}$)	✓	✓	-	✗	✗	-
Feng et al.	✓ ($p_T > 7\,\mathrm{GeV}$)	✓	✗	-	✗	✗	-
Our recent work							
pNRQCD	✓ ($p_T > 5 \times 2m_Q$)	✓	✓	✓(?)	✗	✗	-
Brambilla, Butenschön & **XPW**	✓ ($p_T > 7\,\mathrm{GeV}$)	✓	✓	✓(?)	✗	✓($z < 0.6$)	✓

How should we read the updated score card?

- The failures are now highly localized: large-z photoproduction and other endpoint-sensitive regions.
- Interpretation: the updated global pattern points to endpoint effects as the dominant missing ingredient, rather than a generic failure of NRQCD factorization at low p_T.

4. Summary and Outlook

Question: what have we really learned about where NRQCD works, where it does not, and what the next decisive tests should be?

The remaining puzzles and possible solutions

The remaining tensions mostly coincide with extensions of endpoint regions.

Low-p_T hadroproduction

Possible solution: small-x resummation

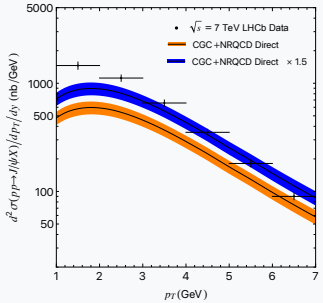

$e^+e^- \to J/\psi X$ at Belle

Possible solution: quarkonium shape function

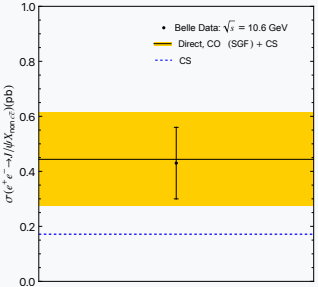

Plots unpublished. SDCs from Ma & Venugopalan, PRL 113, 192301 (2014); Chen, Jin, Ma & Meng, JHEP 03 (2022), 202

Summary and Outlook

Summary

- NRQCD factorization works well for inclusive quarkonium production except in or near endpoint regions, where additional resummations or improved factorization are needed.
- The good description of $\Upsilon(nS)$ production is a highly nontrivial test of the pNRQCD LDME relations.

pp high p_T ($J/\psi, \eta_c, \Upsilon(nS)$, pol.)	$J/\psi + Z$	e^+e^-	γp	$\gamma\gamma$	pp (low p_T, J/ψ)
✓	✓(?)	✓(SGF)	✓($z < 0.6$)	✓	✓ (CGC small-x resum)

Outlook

- More observables to test NRQCD factorization at endpoint region and low-p_T region.
- Shape-function or SGF descriptions for inclusive J/ψ photoproduction at $z > 0.6$.
- Include quarkonium production and polarization in PDF fits.
- The first lattice calculations of CO decay LDMEs in pNRQCD using gradient flow (in preparation).